# Investigation of the Luttinger parameters for InP using hot-electron luminescence

W. Hackenberg, R. T. Phillips, and H. P. Hughes

*University of Cambridge, Cavendish Laboratory, Cambridge CB3 0HE, United Kingdom*

(Received 17 December 1993; revised manuscript received 16 May 1994)

The dispersions of the $\Gamma_6^c$ conduction band and the $\Gamma_8^v$ heavy-hole band in InP are measured with 1-meV accuracy over a range of wave vectors using directionally averaged hot-electron luminescence spectroscopy. The $\mathbf{k} \cdot \mathbf{p}$ method is used to relate wave vectors to the measured energies, and to investigate the sensitivity of these dispersions to the $\mathbf{k} \cdot \mathbf{p}$ parameters in general and to the Luttinger parameters $\gamma_1$, $\gamma_2$, and $\gamma_3$ in particular. It is found that not one but many different Luttinger parameter triplets are consistent with the hot-electron luminescence data, and several works from the literature are reviewed in this new context.

## I. INTRODUCTION

Despite over three decades of study, certain aspects of the electronic structure of InP are not well established, in striking contrast to the situation for GaAs; even the energies of some conduction-band minima are still subject to controversy.[1] The band dispersions in InP have been investigated near high-symmetry points, but with accuracies only of the order of $\sim 10$ meV. Quite small uncertainties of only 1% in the electron and heavy-hole effective masses $m_c^*$ and $m_h^*$ would lead to uncertainties in band energies of several meV near the center of the Brillouin zone [$|\mathbf{k}| \approx 0.05 (2\pi/a)$],[2-8] so it is clear that more detailed investigations of the near-edge band structure of InP at $\Gamma$ are required. Hot-electron luminescence (HEL) spectroscopy[9,10] allows direct measurement of both the electron energy $E_c$ and the heavy-hole energy $E_h$ with an accuracy better than 1 meV over a range of wave vectors in the important central $\Gamma$ valley, and it is therefore appropriate to exploit this technique to study the band structure of InP.

This work presents an investigation of the conduction and heavy-hole bands of bulk InP using a combination of HEL spectroscopy with the $\mathbf{k} \cdot \mathbf{p}$ method of band-structure calculation. Hot-electron to neutral acceptor $(e, A^\circ)$ recombination is used to measure the kinetic *energies* of the heavy-hole $\Gamma_8^v$ band and of the $\Gamma_6^c$ conduction band over a portion of the Brillouin zone not far from its center with 1-meV accuracy, and when the dependence of these kinetic energies on excitation energy is compared with that expected from a $\mathbf{k} \cdot \mathbf{p}$ band structure using commonly accepted parameters, a systematic deviation from the experimental data is discovered. An investigation into this provides an opportunity to improve knowledge of $\mathbf{k} \cdot \mathbf{p}$ parameters for InP by testing them against experiment. The parameters having the most influence on the bands considered are the Luttinger parameters, and this paper concentrates on a critical examination of how the most appropriate Luttinger parameter triplet $(\gamma_1, \gamma_2, \gamma_3)$ can be determined.

## II. THEORY AND EXPERIMENT

Since only the energies of optical transitions are directly accessible by HEL spectroscopy, and the wave vectors only indirectly, we start by plotting the kinetic energies $E_c$ and $E_h$ of the electron and heavy hole involved in a particular excitation versus laser energy $E_{ex}$, from both measurement and calculation. Subsequently we optimize the band-structure calculation and use it to relate the measured energies to wave vectors in order to obtain the $\Gamma_8^v$ and $\Gamma_6^c$ band dispersions.

The hot $(e, A^\circ)$ emission process is summarized here and given in full detail in Ref. 9. Upon cw photoexcitation, one has $E_{ex} = E_h(\mathbf{k}) + E_0 + E_c(\mathbf{k})$, where $E_{ex}$ is the laser energy, $E_h(\mathbf{k})$ the heavy-hole energy, $E_0$ the low-temperature band gap at $\mathbf{k} = 0$, and $E_c(\mathbf{k})$ the kinetic hot-electron energy (direct transitions are assumed). From their point of photoinjection in the conduction band, the hot electrons relax toward the bottom of the band by successive emission of LO phonons on a 100-fs time scale; during this cascade process, a small fraction of the hot electrons recombine with acceptor states by photoluminescence, and this $(e, A^\circ)$ spectrum provides a direct picture of the steady-state energy distribution of the hot-electron population. Figure 1 shows an example of this hot-electron cascade in InP. The peak at highest energy arises from electrons recombining immediately
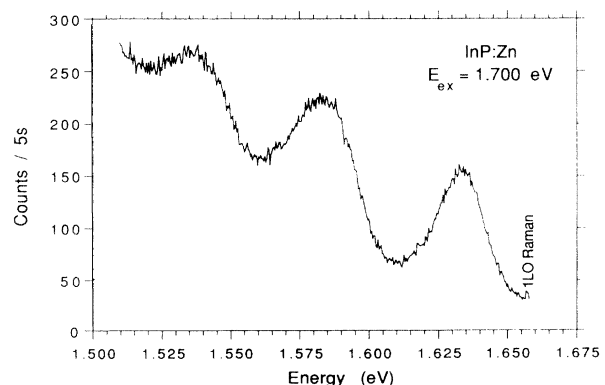
FIG. 1. Hot-electron luminescence cascade in InP:Zn at 6 K under 1.700-eV cw excitation. The peak at highest energy is due to electrons from heavy-hole states; the two lower peaks arise after emission of one and two phonons, but are superimposed here by the light-hole cascade.

   <u>50</u>    10 598   

after excitation from the heavy-hole band and prior to phonon emission. Its luminescence energy is $E_L = E_c(\mathbf{k}) + E_0 - E_a$, where the acceptor binding energy $E_a$ is independent of $\mathbf{k}$ because the acceptors are localized. A similar cascade exists at lower energy from electrons excited from the light-hole band. In Fig. 1 these two cascades overlap from the second peak of the heavy-hole cascade onwards, and hence the peak spacing is different from $\hbar\omega_{LO}$. In the following we focus on the leading peak in the heavy-hole cascade. The kinetic energies (both measured positive with respect to their band extrema) of both the hot electron and the photocreated heavy hole may thus be determined in terms of $E_{ex}$ and

$E_L$, quantities easily accessible from experiment:

$$E_c(\mathbf{k}) = E_L - E_0 + E_a \ ,$$
$$E_h(\mathbf{k}) = E_{ex} - E_L - E_a \ . \tag{1}$$

The corresponding wave vector may of course be found via $E_c(\mathbf{k})$ simply by assuming a parabolic dispersion for the conduction band, as proved useful in Ref. 11, but this is inaccurate on a meV scale; the point of this work is to obtain the dispersions more precisely by taking advantage of the $\mathbf{k}\cdot\mathbf{p}$ method.

The line shape of this hot $(e, A^\circ)$ emission may be calculated[9] for a given $E_{ex}$ with the golden rule:

$$I(E_L) = \int_{\text{Brillouin zone}} d^3k |M_{vc}(\mathbf{k})|^2 |M_{ca}(\mathbf{k})|^2 \delta[E_{ex} - E_c(\mathbf{k}) - E_h(\mathbf{k}) - E_0] \delta[E_L - E_h(\mathbf{k}) - E_0 + E_a] \ . \tag{2}$$

$I(E_L)$ is the total luminescence intensity expected in the $(e, A^\circ)$ spectrum at the energy $E_L$. Energy conservation for excitation and recombination is ensured by the two $\delta$ functions. $E_h(\mathbf{k})$ and $E_c(\mathbf{k})$ are both taken as positive from their band extrema, and a $16 \times 16$ $\mathbf{k}\cdot\mathbf{p}$ Hamiltonian[4] is used for the band structure: it is important that spin-orbit interactions, nonparabolicity, and warping be taken into account when investigating line shapes and polarization effects in any detail. Initially the parameter set suggested in Ref. 4 is used. The optical transition matrix elements $|M_{vc}(\mathbf{k})|^2$ for excitation and $|M_{ca}(\mathbf{k})|^2$ for recombination are calculated in the dipole approximation and depend on the polarizations of the ingoing and outgoing light, and on the carriers' wave vector. Equation (1) is central to the present line shape model: it yields the spectral $(e, A^\circ)$ luminescence profile as it results from the specific $\mathbf{k}\cdot\mathbf{p}$ band structure. For a fit to the measured line shape, the resulting line profile is subsequently broadened by convolution with a Lorentzian.[12]

Measurements were made on a 3-$\mu$m molecular-beam epitaxy (MBE)-grown bulk layer on an InP substrate, with $p < 10^{17}$ cm$^{-3}$ Zn acceptors. At this doping level, the separation between Zn impurities is about 240 Å, compared with the first Bohr radius of 12 Å of an acceptor bound hole in a hydrogenic model;[13] the acceptors are therefore localized and $E_a$ is independent of the wave vector. The sample was kept near 4.2 K, and the incident laser power density well below 10 W/cm$^2$ (corresponding to a density of photoexcited electrons of the order of $10^{14}$ cm$^{-3}$) such that carrier-carrier scattering was insignificant. A dye laser and a Dilor $XY$ spectrometer in a multichannel mode were used, in a $\bar{z}(xy)z$ configuration with $x$, $y$, $z \| [100]$ (i.e. with the incident and luminescence photons with crossed linear polarizations). The band-gap energy $E_0$ was taken to be the sum of the free-exciton recombination energy, measured separately by photoluminescence (PL) and photoluminescence excitation (PLE) spectroscopies, and the published exciton binding energy.[14] The acceptor binding energy $E_a$ was taken to be the difference between the band-gap-related $(e, A^\circ)$ recombination peak and $E_0$. The measured values

$E_0 = (1423.8 \pm 0.2)$ meV and $E_a = (45.6 \pm 0.5)$ meV remained unaffected by changes by factors of 5 in doping level and 100 in laser power.

In order to obtain electron and hole energies $E_h$ and $E_c$ according to Eq. (1), the position $E_L$ of the maximum of the leading peak was measured for a series of laser energies. The result is shown in Fig. 2 as dots. The crosses in
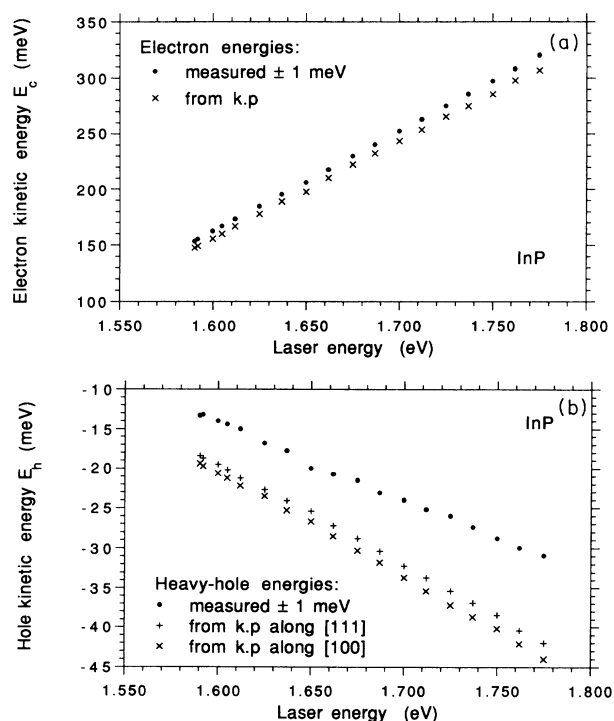


FIG. 2. Plots of the electron energy $E_c$ (upper graph) and the heavy-hole energy $E_h$ (lower graph) as a function of laser energy: ● were obtained from HEL spectra via Eq. (1), + and × from our $\mathbf{k}\cdot\mathbf{p}$ based calculation [Eq. (2)] using the parameters of Table I. The systematic deviation is obvious [$S = 8.4$ meV, cf. Eq. (3)]. As this work shows, other sets of Luttinger parameters would result in a figure similar to this, in agreement to within $\pm 1$ meV.

the same figure represent the energies of those hole and conduction states which were identified in our calculation [cf. Eq. (2)] as taking part in the given excitation and recombination process: this was done by calculating the band structure with $\mathbf{k} \cdot \mathbf{p}$ method for a particular set of Luttinger parameters (Table I) and scanning all wave vectors $\mathbf{k}$ for electron and hole states $E_c(\mathbf{k})$ and $E_h(\mathbf{k})$ between which direct transitions are energetically possible under a given excitation $E_{\mathrm{ex}}$ and which would lead to the measured HEL signal $E_L$. Using Eq. (2) this produced a theoretically luminescence line shape which when suitably broadened with a Lorentzian gives an estimate for $E_L$; together with $E_{\mathrm{ex}}$, this allows $E_c$ and $E_h$ to be obtained from Eq. (1). The effect on $E_L$ of the matrix element is likely to be very small, since spectra taken (for $E_{\mathrm{ex}} < 1.7$ eV) with incident and luminescence photons linearly polarized in parallel (for which the matrix elements are different[12] from those for the crossed configuration used here) have HEL peaks shifted by less than 0.4 meV from those reported here. While the dots are of purely experimental origin, the crosses are semiempirical in that they are based on a $\mathbf{k} \cdot \mathbf{p}$ band structure obtained with the semiempirical parameters of Table I. The discrepancy between the two data sets amounts to 5–10 meV, and far exceeds the resolution of the HEL data. Discrepancies of this order of magnitude can be ignored for some purposes, but it turns out in the following investigation that further knowledge can be gained about the $\mathbf{k} \cdot \mathbf{p}$ parameter set, and a more accurate $E(\mathbf{k})$ diagram can be drawn, by exploiting such high-resolution HEL data.

Based on the considerations made by Cardona, Christensen, and Fasol [who compared the $\mathbf{k} \cdot \mathbf{p}$, linear muffin-tin orbital (LMTO), and local-density-approximation (LDA) methods, and empirical data[4]] we set out on the assumption that the $\mathbf{k} \cdot \mathbf{p}$ method can produce meaningful band dispersion over the range 0.04 to 0.08 $(2\pi/a)$ of wave vectors probed by the present experiment. Some of the parameters required (cf. Table I) are easily accessible by measurement, such as the lattice constant and the fundamental band gap; others even today still carry large uncertainties, such as the splitting $\Gamma_8^c - \Gamma_7^c$, for which values different by a factor of 7 are found in the literature.

## III. SENSITIVITY OF THE BAND DISPERSIONS TO $\mathbf{k} \cdot \mathbf{p}$ PARAMETERS

Each parameter entering the $\mathbf{k} \cdot \mathbf{p}$ matrix was investigated for its effect on the $\Gamma_6^c$ conduction and $\Gamma_8^c$ heavy-hole dispersions using a method previously applied to magneto-Raman-scattering data.[15] Starting with the set of values suggested by Cardona, Christensen, and Fasol,[4] each parameter was varied in about 20 small increments over a chosen range around its suggested value, and an entire band structure was computed each time, while all other parameters entering the calculation were constant. Then, as above, a pair of kinetic energies $E_c^{\mathrm{calc}}$ and $E_h^{\mathrm{calc}}$ was determined on the basis of that one particular dispersion for each of the $N = 18$ excitation energies experimentally used. This way a graph analogous to Fig. 2 is obtained, where the calculated set of 18 pairs of energies can be compared to the 18 pairs of measured $E_c^{\mathrm{meas}}$ and $E_h^{\mathrm{meas}}$. The following figure of merit $S$ was defined in order to quantify the overall discrepancy between the two data sets obtained with each of the numerous $\mathbf{k} \cdot \mathbf{p}$ parameter sets put to test. It represents, in units of meV, the average difference between corresponding calculated and measured energies:

TABLE I. Set of $\mathbf{k} \cdot \mathbf{p}$ parameters for InP used in the $16 \times 16$ Hamiltonian. The second column lists their values given in Ref. 4, the third gives the ranges over which they are investigated in the present work (increments are given in parentheses, within which no fine structure was found). The partial derivatives in the fourth column are a measure of the sensitivity of the conduction and heavy-hole band dispersions to each of the $\mathbf{k} \cdot \mathbf{p}$ parameters [cf. Eq. (3)]. The results are discussed in the text.

| Parameters, $p_i$ | Values from Ref. 4 | Investigated range (increment) | $\partial S / \partial p_i$ |
|---|---|---|---|
| $E_0$ (eV) | 1.4238 | | |
| $\Delta_0$ (eV) | 0.108 | 0.100–0.119 (0.001) | $\approx 0$ |
| $E_0'$ (eV) | 4.6 | 4.40–4.85 (0.05) | $\approx 0$ |
| $\Delta_0'$ (eV) | 0.5 | 0.07–1 (0.05) | $-2.7$ meV/100 meV |
| $\Delta^-$ (eV) | 0.22 | 0.1–1 (0.05) | has a minimum, see text |
| $E_0'''$ (eV) | 9.66 | 7.6–11.4 (0.02) | $\approx 0$ |
| $P$ (eV Å) | 8.65 | 7–10 (0.1) | $-7$ meV/0.25 eV Å |
| $P'$ (eV Å) | 4.31 | 2–6.75 (0.1) | $+2.4$ meV/0.25 eV Å |
| $P'''$ (eV Å) | 3.50 | 1.5–5.3 (0.1) | $\approx 0$ |
| $Q$ (eV Å) | 7.24 | 5–9.75 (0.1) | $-8$ meV/0.25 eV Å |
| $C_k$ ($10^{-3}$ eV Å) | $-1.44$ | $(-2)$–$(-1)$(0.05) | $\approx 0$ |
| $C_k'$ ($10^{-3}$ eV Å) | $-1.15$ | $(-1.3)$–$(0.9)$ (0.05) | $\approx 0$ |
| $\gamma_1$ | 5.05 | 3–5.8 | cf. Fig. 3(a) |
| $\gamma_2$ | 1.6 | 0.6–2.5 | cf. Fig. 3(b) |
| $\gamma_3$ | 1.73 | 0.7–2.7 | cf. Fig. 3(c) |
| $a$ (Å) | 5.869 | | |

$$S^2 = \frac{1}{2N} \sum_{i=1}^{18} [E_c^{\text{calc};i} - -E_c^{\text{meas}})^2 + (E_h^{\text{calc};i} - E_h^{\text{meas}})^2] \ . \quad (3)$$

In this sum over variances, the two measured quantities are not independent of each other [cf. Eq. (1)], but it still proved a practical way of judging the adequacy of the parameter set in question. For example, with the original parameter set (Table I), $S = 8.4$ meV, meaning that the average deviation of the calculated from the measured energy on a graph like that of Fig. 2 is 8.4 meV. Note that $S = \sqrt{S^2}$ does not give the direction of the deviation. The small this figure of merit $S$, the better the agreement between the calculated conduction and heavy-hole bands with HEL data over the measured range. Due to the spectral resolution, the smallest meaningful value for $S$ is not much less than 1 meV.

At this point, however, we are not yet interested in the minimization of $S$, but in observing its behavior as each parameter is varied. The range of values tested for each parameter is also given in Table I; it was chosen arbitrarily to cover most values found in the literature. Note that while it is certainly an advantage of this technique that not just one point but a significant portion of the $\Gamma_6^c$ and heavy $\Gamma_8^v$ bands is thus put to a test, effects on other bands are ignored by this technique. The results of this procedure, listed in the last column of Table I, may be divided into three categories in terms of the bands' sensitivity to them: (i) insensitive, when $\partial S / \partial p_i \approx 0$; (ii) monotonically sensitive, when $\partial S / \partial p_i > 0$ or $\partial S / \partial p_i < 0$; and (iii) critical, when $\partial S / \partial p_i$ exhibits a minimum. Definitions of these parameters and an extensive discussion may be found in Ref. 4.

The parameters to which $S$ is relatively insensitive over the specified range are $\Delta_0$, $E_0'$, $E_0'''$, $P'''$, $C_k$, and $C_k'$. Neither the heavy-hole band $\Gamma_8^v$ nor the lowest conduction band $\Gamma_6^c$ are expected to be influenced strongly by interactions with bands as distant as $\Gamma_7^c$ and $\Gamma_6^{c'}$, and therefore their insensitivity to the corresponding energy gaps $E_0'$ and $E_0'''$ and to the overlap integral $P'''$ is not surprising. $C_k$ and $C_k'$ are the coefficients of terms linear in $k$ in the Hamiltonian matrix, giving rise to spin splittings linear in $k$ for the $\Gamma_8^v$ and $\Gamma_6^c$ states, respectively. Because the latter band is relatively remote, $C_k'$ in any case contributes less to $\Gamma_8^v$ than does $C_k$. The fact that the heavy-hole band seems to be insensitive to its own $k$-linear terms weighted by $C_k$ may be explained by the Kramers degeneracy, and the fact that any spin splittings will average out in an isotropic measurement or calculation. Given that it is well established that $\Delta_0 = (108 \pm 1)$ meV,[8,14] $\partial S / \partial \Delta_0 \approx 0.7$ meV/meV is ignored. Similarly, the well-established fundamental band gap $E_0$ and lattice constant $a$ have not been varied.

The group of parameters to which $S$ is monotonically sensitive, i.e., for which $\partial S / \partial p_i$ is either positive or negative over the given range, consists of $\Delta_0'$, $P$, $P'$, and $Q$. The parameter $P$ is determined as a function of the known conduction-band effective mass at $\Gamma_6^c$, of $E_0$ and $\Delta_0$ (which by themselves do not affect $S$) and of $P'$. In turn, $P'$ is determined from a relationship between $P$, $E_0'$,

and the $\Gamma_{15}$-$\Gamma_1$ gap of the isoelectronic group-IV material Ge.[4] The determination of these quantities is not investigated anew here, but it is noted that seemingly extreme values would be needed to make $S$ vanish, namely $P \approx 10^{-9}$ eV cm and $P' \approx 10^{-8}$ eV cm. The parameter $Q$, which couples the $p$-type valence to the $p$-type conduction bands, is a function of $\gamma_1$, $\gamma_2$, $E_0'$, and $\Delta_0'$; whereas $E_0'$ does not affect $S$, the Luttinger parameters do, as will be discussed below. Wide discrepancies show in the value of $\Delta_0'$: whereas Cardona, Christensen, and Fasol calculate a value of 500 meV with the LMTO method, others have found a room-temperature value of 70 meV.[16] A very large value of 1.6 eV would be necessary for $S$ to reach zero, and it therefore seems safe, here too, to assume the earlier value of 0.5 eV and to search elsewhere for critical parameters. The spin-orbit parameter $\Delta^-$, coupling the $\Gamma_{15}^c$ and $\Gamma_{15}^v$ bands, was taken as $\Delta^- = 0.22$ eV, after k·p, local combination of atomic orbitals (LCAO), and LMTO
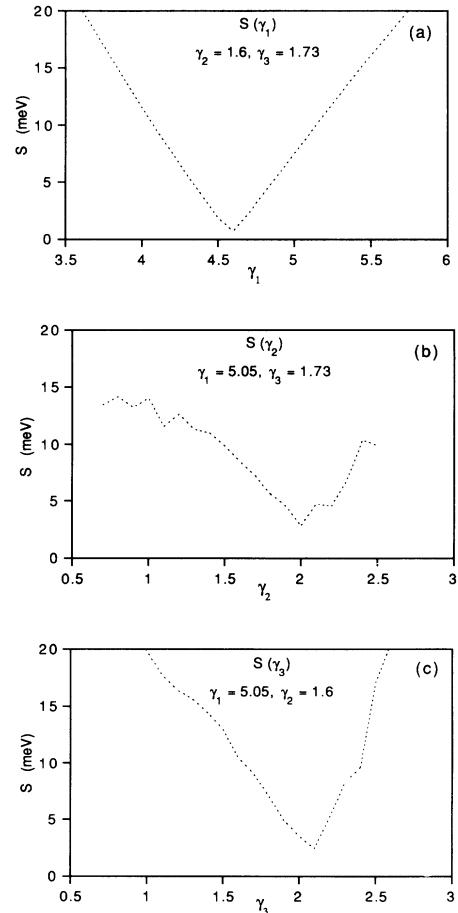


FIG. 3. Sensitivity of the figure of merit $S$ in Eq. (3) to the Luttinger parametes $(\gamma_1, \gamma_2, \gamma_3)$ when all other k·p parameters have the values given in Table I. This shows that a small variation of $\gamma_1$ within realistic bounds can minimize $S$ and thus bring the k·p bands into agreement with the measured HEL data. For example, the triplet (5.05, 1.6, 173) suggested in Ref. 4 yields an average discrepancy $S = 8.4$ meV (see Fig. 2), whereas substituting $\gamma_1 = 4.6$ is shown in (a) to lead to much better agreement at $S \approx 1$ meV.

calculations had given values of 0.4, 0.16, and 0.226 eV, respectively.[4] In the range 0.1 to 1 eV, $\partial S/\partial\Delta^-$ has a minimum near 0.45 eV with $S=8$ meV, and varies only slowly at about 1.6 meV/0.1 eV. This large value of $S$, indicating bad agreement with the experiment, and its being relatively insensitive to $\Delta^-$, suggest that, in the absence of other evidence, the original choice be adhered to.

Finally, when the Luttinger parameters $\gamma_1$, $\gamma_2$, and $\gamma_3$ are investigated, one finds that $S$ is very critically dependent on their values. Figure 3 shows distinct minima of the partial derivatives $\partial S/\partial\gamma_1$. Interestingly, these minima occur at values of each of the $\gamma_1$ within the range commonly quoted for InP. Thus a change of any one of the three Luttinger parameters (5.05, 1.6, and 1.73) suggested in Ref. 4 and considered in Fig. 3, without having to be considered extreme, would be sufficient for the present $\mathbf{k\cdot p}$ calculation to yield a conduction and valence band agreeing completely with the measured HEL data. This is the case with none of the other $\mathbf{k\cdot p}$ parameters. It is therefore interesting to focus on the Luttinger parameters.

## IV. THE LUTTINGER PARAMETERS

In a general form Luttinger derived the spin-orbit Hamiltonian for the fourfold degenerate hole level at the top of the valence band.[17] In its field-independent terms three dimensionless material constants $\gamma_1$, $\gamma_2$, and $\gamma_3$—the Luttinger parameters—appear in expressions for $E(\mathbf{k})$ that describe the heavy and light effective-mass valence bands of semiconductors. The magnitude of these parameters has to be found empirically.

In the present work, in order to determine the optimal set $(\gamma_1, \gamma_2, \gamma_3)$ that minimizes the sum $S$ of the variances between the measured and calculated electron and hole energies [Fig. 2 and Eq. (3)], $S$ was calculated as a function of $(\gamma_1, \gamma_2, \gamma_3)$ over a wide range for each parameter. The result is a three-dimensional scalar array of $S$ with axes $\gamma_i$. First a large coarse grid of 3640 points was used $(4.4 \leq \gamma_1 \leq 6.3, 1.0 \leq \gamma_2 \leq 2.3, 1.6 \leq \gamma_3 \leq 2.8$, step 0.1), and subsequently a smaller and finer grid of 2940 points $(4.70 \leq \gamma_1 \leq 5.09, 1.60 \leq \gamma_2 \leq 1.99, 1.72 \leq \gamma_3 \leq 2.14$, step 0.03).

The interest lies in determining the points in $\gamma$ space where $S(\gamma_1, \gamma_2, \gamma_3)$ is minimal, since this is the condition for the Luttinger parameters, in conjunction with the unaltered remaining $\mathbf{k\cdot p}$ input, to generate bands that match the experimental points on the $E_c(\mathbf{k})$-versus-$E_{ex}$ and $E_v(\mathbf{k})$-versus-$E_{ex}$ graphs. It turns out that the sets of $(\gamma_1, \gamma_2, \gamma_3)$ for which $S \leq 1$ meV lie roughly within a long cylindrical volume in $\gamma$ space, oriented along a diagonal of a cube enclosing the second, finer grid, as represented schematically in Fig. 4: any set of Luttinger parameters that represent the coordinates of a point within this darkened shape, together with the other parameters of Table I, produces a $\mathbf{k\cdot p}$ band structure of InP that agrees to within experimental and numerical accuracy with the HEL data. Cross sections (or slices) through this volume are given quantitatively in Table II. It thus appears from the spatial extent of the set of Luttinger parameters
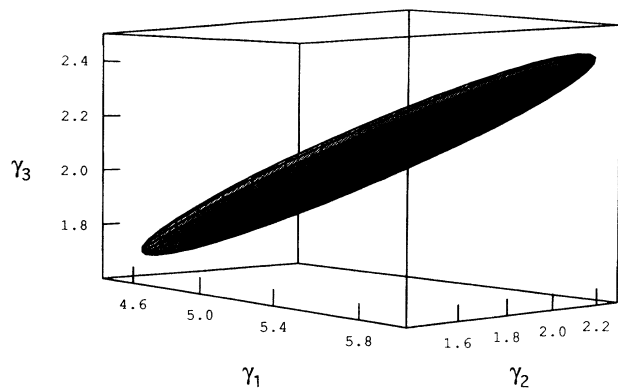


FIG. 4. Schematic representation of the volume in Luttinger space, where $(\gamma_1, \gamma_2, \gamma_3)$ lead to $S \leq 1$ meV, i.e., to good agreement with the HEL data. Clearly, Luttinger parameters of significantly different magnitudes do not necessarily contradict neither each other or the present HEL measurements.

$(\gamma_1, \gamma_2, \gamma_3)$ in Fig. 4 that there is not one well-defined triplet, but that a large number of triplets is compatible with the $\mathbf{k\cdot p}$ method and with HEL spectroscopy.

Table III explicitly lists some of the Luttinger parameter triplets which are identified in this manner as being consistent with the HEL data. Given the fineness of the grids used, it should give a useful idea of other permitted values by interpolation. The small anisotropy (e.g., $\gamma_3-\gamma_2$) means that a much larger anisotropy is not compatible with the HEL linewidth. Since these results are derived over many different wave vectors, the heavy-hole band in InP is not much more anisotropic than the difference $\gamma_3-\gamma_2 \leq 0.2$ implies. Luttinger parameters where $\gamma_3-\gamma_2 \geq 0.4$ thus seem unlikely [although the set used below for Fig. 6(e) might suggest a larger anisotropy, a much worse fit is obtained at larger wave vectors; $S=4.4$ meV is an average]. However, this investigation does not resolve the direction of the carrier momentum, which would be expected to clarify this point.[18]

Finally, Fig. 5 shows two pairs of heavy-hole and conduction bands for InP obtained with two Luttinger parameter sets taken from either end of Table III [(6.0, 2.3, and 2.5) and (4.6, 1.6, and 1.73)], all other parameters required for the $\mathbf{k\cdot p}$ calculation being identical to those in Table I. The three main inputs used to obtain these dispersions were the band separation at $\mathbf{k}=0$, 18 pairs of energies of simultaneously measured conduction and heavy-hole states at wavevectors between 0.04 and 0.08 $(2\pi/a)$, and the $16\times16$ $\mathbf{k\cdot p}$ calculation optimized in terms of Luttinger parameters by use of the expression $S$ to fit the HEL measurements. Since the $\gamma_i$, on which these bands are based, fulfill the criterion $S \leq 1$ meV, both pairs of bands are consistent with the hot luminescence spectra at all 18 excitation energies, but the wavevector region in which the optical transitions would have taken place between the less dispersive bands is shifted to larger $k$ compared to the transitions between more dispersive bands. Figure 5 thus illustrates the difficulty of relating energies to wave vectors (often avoided by as-

TABLE II. Table of values (in meV) of the expression $S$ of Eq. (3) for various values of the parameters $(\gamma_1,\gamma_2,\gamma_3)$; the three parts of the table represent cross sections through the schematic volume of Fig. 4 corresponding to $\gamma_1=4.5$, $\gamma_2=1.5$, and $\gamma_3=1.7$. Best agreement between the calculated InP bands and the HEL data in the sense of Fig. 2 is obtained when $(\gamma_1,\gamma_2,\gamma_3)$ are chosen such that $S\le 1$ (i.e., $\gamma_1=4.5$, $\gamma_2=1.5$, and $\gamma_3=1.7$).

$\gamma_1=4.5$

| $\gamma_3\downarrow$ | 1.3 | 1.4 | 1.5 | 1.6 | 1.7 | 1.8 $\leftarrow\gamma_2$ |
|---|---|---|---|---|---|---|
| 2.0 | . | . | . | . | . | . |
| 1.9 | . | 9 | . | . | . | . |
| 1.8 | 5 | 4 | 6 | 7 | . | . |
| 1.7 | . | 3 | 1 | 2 | 5 | . |
| 1.6 | . | 8 | 6 | 3 | 2 | . |

$\gamma_2=1.5$

| $\gamma_1\downarrow$ | 1.6 | 1.7 | 1.8 | 1.9 | 2.0 | 2.1 | 2.2 | 2.3 $\leftarrow\gamma_3$ |
|---|---|---|---|---|---|---|---|---|
| 5.2 | . | . | . | . | . | . | . | . |
| 5.1 | . | . | . | . | . | . | 9 | . |
| 5.0 | . | . | . | . | 6 | 7 | . | . |
| 4.9 | . | . | . | 5 | 6 | . | . | . |
| 4.8 | . | . | 7 | 6 | 6 | . | . | . |
| 4.7 | . | 8 | 5 | 6 | 6 | . | . | . |
| 4.6 | 9 | 5 | 3 | 7 | . | . | . | . |
| 4.5 | 6 | 1 | 6 | . | . | . | . | . |
| 4.4 | 2 | 4 | 8 | . | . | . | . | . |

$\gamma_3=1.7$

| $\gamma_1\downarrow$ | 1.1 | 1.2 | 1.3 | 1.4 | 1.5 | 1.6 | 1.7 | 1.8 | 1.9 | 2.0 | 2.1 | 2.2 | 2.3 $\leftarrow\gamma_2$ |
|---|---|---|---|---|---|---|---|---|---|---|---|---|---|
| 5.3 | . | . | . | . | . | . | . | . | . | . | . | . | . |
| 5.2 | . | . | . | . | . | . | . | . | . | . | . | 8 | . |
| 5.1 | . | . | . | . | . | . | . | . | . | 7 | 8 | 8 | . |
| 5.0 | . | . | . | . | . | . | . | . | 8 | 7 | . | 9 | . |
| 4.9 | . | . | . | . | . | . | . | 7 | 5 | 5 | 8 | . | . |
| 4.8 | . | . | . | . | . | . | 6 | 4 | 3 | 9 | . | . | . |
| 4.7 | . | . | . | . | 8 | 6 | 4 | 4 | 7 | . | . | . | . |
| 4.6 | . | . | . | 8 | 5 | 2 | 3 | 6 | 9 | . | . | . | . |
| 4.5 | 9 | . | . | 3 | 1 | 2 | 5 | . | . | . | . | . | . |
| 4.4 | . | 7 | 3 | 3 | 4 | 6 | . | . | . | . | . | . | . |

suming parabolicity), giving the dispersions for the conduction and heavy-hole band of InP over a wide range of $k$ near $\Gamma$. The two conduction-band masses are both $0.08m_0$ near $k=0$ and increase to $0.09m_0$ at $k=0.06(2\pi/a)$, when obtained numerically through $m^*=p/v_g=\hbar^2k/(dE/dk)$. The two heavy-hole masses are identical near $k=0$ ($m^*_{[100]}=0.82m_0$ and $m^*_{[111]}=0.87m_0$; no HEL data exist near this point). Near $k=0.06$ $(2\pi/a)$, and when using $m^*_{[100]}=(\gamma_1-2\gamma_2)^{-1}m_0$, they are also equal, but the effective masses differ in the [111] directions, for which $m^*_{[111]}=(\gamma_1-2\gamma_3)^{-1}m_0$ yields values of $0.88m_0$ and

$1.0m_0$. This illustrates how the relatively high resolution of HEL has revealed the *insensitivity* of effective-mass values to Luttinger parameters, particularly when measured or derived for limited wave-vector regions.

## V. COMPARISON WITH OTHER WORK

Since previously published work concerned with this topic usually determines, or makes use of, a single triplet, this section discusses some of the Luttinger parameters found in the literature in the light of the above study (Table IV). Serious inconsistencies among them are re-

TABLE III. Some of the Luttinger parameters ($\pm 0.02$) identified by the criterion $S\le 1$ meV to yield agreement with the HEL data. All these points lie within the volume depicted in Fig. 4 and yield the same agreement with the HEL data over the wave-vector range considered as that shown in Fig. 6(f). The list is not complete, since the stepwidth is set arbitrarily in the grids of Sec. III.

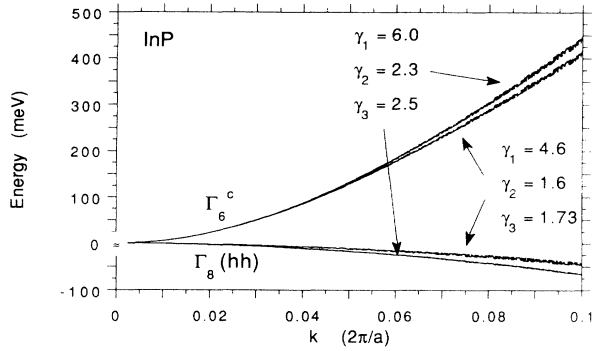| $\gamma_1$ | 4.5 | 4.6 | 4.7 | 4.8 | 4.9 | 5.1 | 5.2 | 5.4 | 5.7 | 5.8 | 6.0 |
|---|---|---|---|---|---|---|---|---|---|---|---|
| $\gamma_2$ | 1.5 | 1.6 | 1.6 | 1.8 | 1.8 | 1.9 | 2.0 | 2.1 | 2.2 | 2.3 | 2.3 |
| $\gamma_3$ | 1.7 | 1.73 | 1.8 | 1.8 | 1.9 | 2.0 | 2.0 | 2.1 | 2.3 | 2.3 | 2.5 |

FIG. 5. Conduction and heavy-hole bands calculated with the k·p method for InP with two sets of Luttinger parameters, taken from both ends of Table III, where $S \leq 1$ meV. Both pairs of bands are thus consistent with HEL, but the optical transitions would have occurred at slightly differing k. The triplet (4.6, 1.6, 1.73) is based on the values used in Ref. 4 and optimized according to Fig. 3(a).

vealed if, for example, the anisotropy of the heavy-hole band is calculated: using the expressions for $m^*_{[100]}$ and $m^*_{[111]}$ in Sec. IV, the nearly equal $\gamma_2$ and $\gamma_3$ of Leotin et al. produce nearly isotropic bands with a mass ratio of 1.2, whereas Bimberg et al. predict a highly anisotropic band mass ratio of 6.6. All but the last two triplets of Table IV were tested for consistency with the HEL data in the above manner; the future of merit $S$ obtained for every set $(\gamma_1, \gamma_2, \gamma_3)$ is given in the last column. One notices that similarly good agreement with the present range of HEL data is achieved with quite different sets of Luttinger parameters (e.g., the Alekseev and Dean data), while other numbers which appear to be in line with the rest disagree more strongly with the present measurements (e.g., the Bimberg and Cardona data). As some values were determined from theoretical considerations, and others experimentally for one particular wave vector, this illustrates the usefulness of testing the Luttinger parameters using optical results at 1-meV resolution over an entire range of wave vectors.

Taking a different perspective, the hot luminescence line shapes are now calculated for a single $E_{ex}$ (corresponding to one narrow k interval) for some of the sets $(\gamma_1, \gamma_2, \gamma_3)$ from Table IV. In contrast to $S$, which is a figure of merit averaged over a large portion of the bands,

only one point is thus sampled, but it illustrates well the point of this study. $E_{ex} = 1.650$ eV is taken, corresponding to hot electron energies around 200 meV. In Fig. 6, the calculated luminescence profile is given in both its unbroadened and broadened form against the background of the measured spectrum for six different Luttinger triplets. For a best fit to measurement, each of the unbroadened profiles was convoluted with a Lorentzian using as a broadening parameter $\sigma = 8$ meV, except for the wide profiles in Figs. 6(b) and 6(e) where $\sigma = 6$ meV was used. The Luttinger parameters in Figs. 6(a)–6(e) are taken from Table IV, and that in Fig. 6(f) from one of the sets identified as consistent with HEL data above (cf. Figs. 4–6). The effect of individual Luttinger parameters on the HEL spectrum can be read from the unbroadened profiles. For example, the difference $\gamma_1 - 2\gamma_2$ determines the heavy-hole band dispersion along [100], and therefore the lower-energy limit of the profiles in Figs. 6(a) and 6(c) is almost identical; since the difference $\gamma_3 - \gamma_2$ determines the band anisotropy, the same profiles have different widths. Lifetime considerations could, in principle, place bounds on the band anisotropy, if the hot-electron lifetime and other spectral broadening mechanisms were known; if 3–4 meV were attributable to lifetime broadening, a hot-electron lifetime $\tau \approx 120-160$ fs is obtained, which is consistent with known figures for GaAs.

The widely varying degree of agreement between the calculated and measured line shapes is obvious. However, even very different Luttinger triplets can produce remarkably similar spectral line shapes, such as those due to Alekseev et al. in Fig. 6(a) and Dean, Robbins, and Bishop in Fig. 6(d). This only happens to be so at this small k interval set by the arbitrary choice of $E_{ex}$; the magnitude of $S$ is a better indication for the more relevant agreement over a large k range. This indicates again that Luttinger parameters ought to be derived from large wave-vector ranges if their validity is not to be restricted to particular points in the band diagram, the location of which is determined by the technique in the particular investigation.

The spectrum in Fig. 6(f) delivers the best agreement. The Luttinger triplet used is $(\gamma_1 = 4.6, \gamma_2 = 1.6,$ and $\gamma_3 = 1.73)$ and is based on the original set suggested by Cardona, Christensen, and Fasol, but altered in $\gamma_1$ according to the minimum in $S(\gamma_1)$ revealed in Fig. 3. Since $S = 1$ meV, this set gives agreement with the HEL

TABLE IV. A selection of Luttinger parameters found in the literature and discussed in Sec. V. Numbers in parentheses are used, rather than those determined, by the authors. The last column gives the value of $S$ in each case as defined in Eq. 3. The names are those of the first authors in Refs. 2–8. See also Fig. 6.

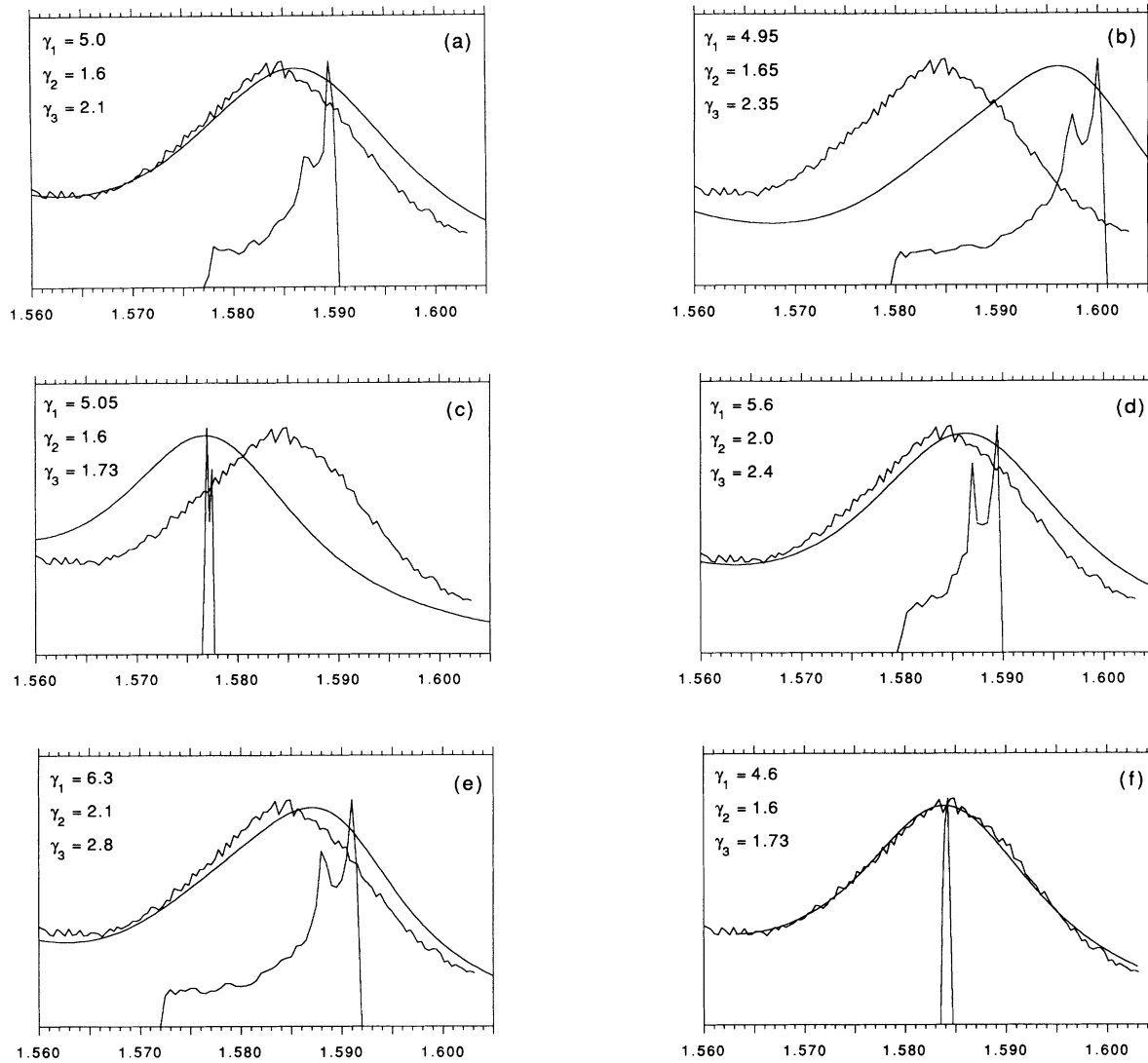| Reference | $\gamma_1$ | $\gamma_2$ | $\gamma_3$ | $S$ (meV) |
|---|---|---|---|---|
| Alekseev et al. | (5.0) | (1.6) | 2.10±0.1 | 3.0 |
| Bimberg et al. | 4.95±0.2 | 1.65±0.2 | 2.35±0.2 | 13.0 |
| Cardon, Christensen, and Fasol | (5.05) | (1.6) | (1.73) | 8.4 |
| Dean, Robbins, and Bishop | 5.6±0.7 | 2.0±0.3 | 2.4±0.4 | 2.9 |
| Lawaetz | 6.3 | 2.1 | 2.8 | 4.4 |
| Leotin et al. | 5.04±0.1 | 1.56±0.03 | 1.73±0.03 | |
| Rochon and Fortin | 5.15±0.05 | 0.94±0.03 | 1.62±0.03 | |

FIG. 6. Comparison of a HEL spectrum measured at 1.650 eV with profiles calculated with the k·p parameters of Table I and six different sets of Luttinger parameters. In each graph, the spiky shape is the calculated *unbroadened* profile after Eq. (2); the smooth curve is after convolution with a Lorentzian. The values for $(\gamma_1, \gamma_2, \gamma_3)$ are taken from: (a) Alekseev *et al.* (Ref. 2) (b) Bimberg *et al.* (Ref. 3); (c) Cardona, Christensen, and Fasol (Ref. 4); (d) Dean, Robbins, and Bishop (Ref. 5); (e) Lawratz (Ref. 6); (f) is a typical fit for all values of Table III.

data not only at the specific $E_{ex}$ illustrated in this figure, but at each of the 18 excitation energies probed in Sec. III, i.e., throughout the wave-vector region 0.04–0.08 $(2\pi/a)$. Fits virtually indistinguishable from that in Fig. 6(f) are obtained when any other Luttinger parameters are selected from within the shaded volume of Fig. 4, e.g. (4.5, 1.5, 1.7) or (6.0, 2.3, 2.5), since each meets the condition $S \leq 1$ meV, illustrating the consistency of the present method and the fact that many sets $(\gamma_1, \gamma_2, \gamma_3)$ are compatible with HEL spectroscopy.

Alekseev *et al.* fixed $\gamma_1 = 5.0$ and $\gamma_2 = 1.6$ after Refs. 3 and 7, and determined $\gamma_3$ from the degree of linear polarization of HEL in InP:Zn at $E_{ex} = 1.959$ eV.[2] The validity at large k of the triplet obtained is assumed implicitly. Bimberg *et al.* determine the complete set of Luttinger parameters from reflectance experiments in which they

measure the energy levels of free excitons in magnetic fields up to 20 T.[3] These values were determined near the band gap and do not necessarily contain information about the band dispersion away from k=0. Conversely, the present method was developed over a wave-vector range away from the Γ point, so that the disagreement in Fig. 6(b) does not necessarily imply a contradiction. While it remains unclear how the magnitude of the error bars was determined, Bimberg *et al.* make an observation particularly interesting in this context. They test their Luttinger parameters by using them to calculate the acceptor binding energy and find a value of 54 meV, seemingly incompatible with the 46 meV measured earlier by one of the authors, and they point out that a change in $\gamma_1$ of just 0.15 is sufficient to resolve this incompatibility. This shows the difficulty of determining the Luttinger pa-

rameters from only one type of measurement.

Cardona, Christensen, and Fasol chose the Luttinger parameters in Table I for their $16 \times 16$ k·p Hamiltonian.[4] Doing so yields the spectra in Fig. 6(c), with which the measured spectrum is clearly not compatible. If, for example, $\gamma_1$ is altered to 4.6 and $\gamma_2$ and $\gamma_3$ remain unchanged, a good fit to all 18 measurements is achieved with $S = 0.7$ meV, illustrated in Fig. 6(f). Dean, Robbins, and Bishop derive all three $\gamma_i$'s from PL and PLE spectra of excited acceptor states together with some theoretical input, allowing for large errors;[5] nevertheless good results are obtained with the values (5.6, 2.0, 2.4) quoted, reflected in $S = 2.9$ meV, and in Fig. 6(d). Lawaetz used a five-level k·p calculation to determine the valence-band parameters for a large number of cubic semiconductor materials at $k = 0$, making use of four semiempirical parameters for Ge, one for $\alpha$-Sn and a general one for III-V compounds.[6] Despite the very large $\gamma_i$ given in this early work, reasonable agreement with HEL is found in Fig. 6(e) and for $S$ (Table IV). Leotin et al. observed cyclotron resonance absorption from thermal holes in $p$-type material at 110 K under 337-$\mu$m excitation as a function of pulsed magnetic fields up to 35 T.[7] They determined the effective heavy- and light-hole masses in the [100] and [111] directions and indirectly the Luttinger parameters. Their values are very similar to those of Cardona, Christensen, and Fasol, and yield a result very similar to that in Fig. 5(c). Comparability is limited, however, due to valence-band mixing in a magnetic field. Rochon and Fortin used the photovoltaic effect and reflectivity measurements in magnetic fields up to 7 T to measure energies of excitons associated with Landau levels up to $n = 10$.[8] Fitting the fan plots obtained with the Pidgeon-Brown theory allowed them to determine $\gamma_1$ and $\gamma_2$. One of their boundary conditions was $\gamma_2 - \gamma_3 = 0.7$ after Ref. 6, and it is mainly because of this constraint that the k·p method produces an HEL spectrum outside the window of Fig. 6.

In summary, other workers have produced Luttinger parameters that differ widely in magnitude and in the implied anisotropy of the conduction and heavy-hole bands, and the k regions for which their results are thought to be valid is unclear. When these values are tested for consistency with the present HEL data over a range of 170 meV in electron energies, it is found that although none are compatible with the present HEL data to within 1 meV, most are in reasonable agreement with each other and with the measurements. This suggests that markedly different sets of Luttinger parameters do not necessarily contradict each other. In this context it should be emphasized that the measurements presented here are directionally averaged and involve a wide range of values of $k$

(0.04 to 0.08 $2\pi/a$), and the Luttinger parameters involved thus implicity trade off goodness of fit in one region of k space with that in another. Fitting data for a more constrained region (i.e. over a narrower energy range and involving directional selection[18]) may produce better defined sets of parameters, but parameters which would be less generally applicable and which would still have been determined for a given set of semiempirical k·p parameters. Although in principle better values for the Luttinger parameters could thus be obtained for small ranges of k, the present approach has the advantage of providing sets of Luttinger parameters which are good at describing the band structure over a reasonably wide range of k space.

## VI. CONCLUSION

The energies of $\Gamma_6^c$ conduction-band states and $\Gamma_8^v$ heavy-hole states in InP have been measured with 1-meV accuracy over a range of directionally averaged wave vectors between 0.04 and 0.08 ($2\pi/a$) using hot $(e, A°)$ luminescence spectroscopy. In order to draw the $E(\mathbf{k})$-band dispersions, the corresponding wave vectors were determined using a $16 \times 16$ k·p band-structure calculation. In doing so, the sensitivity of these dispersions to the Luttinger parameters $\gamma_1$, $\gamma_2$, and $\gamma_3$ was studied. A range of Luttinger parameter triplets $(\gamma_1, \gamma_2, \gamma_3)$ has been identified to be consistent with the HEL data, all suggesting moderately warped bands. Several published works about Luttinger parameters have been briefly reviewed and while none of them is consistent with the present hot luminescence measurements to within 1 meV, it has been established here that seemingly very different triplets of Luttinger parameters $(\gamma_1, \gamma_2, \gamma_3)$ do not necessarily contradict each other. The most serious weaknesses of the band-structure investigation presented (and thus of the conclusions drawn about the Luttinger parameters) are its reliance so far on other semiempirical parameters and the inability to probe at $k = 0$ by the same technique; its most significant strengths are the high experimental accuracy and the coverage of a relatively wide range of wave vectors.

[1]J. Peretti, H.-J. Drouhin, D. Paget, and A. Mircéa, Phys. Rev. B **44**, 7999 (1991).

[2]M. A. Alekseev, I. Y. Karlik, I. A. Merkulov, D. N. Mirlin, and V. F. Sapega, Phys. Lett. A **127**, 373 (1988).

[3]D. Bimberg, K. Hess, N. O. Lipari, J. U. Fischbach, and M.

Altarelli, Physica **89B**, 139 (1977).

[4]M. Cardona, N. E. Christensen, and G. Fasol, Phys. Rev. B **38**, 1806 (1988).

[5]P. J. Dean, D. J. Robbins, and S. G. Bishop, Solid State Commun. **32**, 379 (1979).

[6]P. Lawaetz, Phys. Rev. B **4**, 3460 (1971).

[7]J. Leotin, R. Barbaste, S. Askenazy, M. S. Skolnick, R. A. Stradling, and J. Tuchendler, Solid State Commun. **15**, 693 (1974).

[8]P. Rochon and E. Fortin, Phys. Rev. B **12**, 5803 (1975).

[9]G. Fasol, W. Hackenberg, H. P. Hughes, E. Bauser, K. Ploog, and H. Kano, Phys. Rev. B **41**, 1461 (1990).

[10]J. A. Kash, Phys. Rev. B **47**, 1221 (1993).

[11]G. Fasol and H. P. Hughes, Phys. Rev. B **33**, 2953 (1986).

[12]W. Hackenberg, H. P. Hughes, G. Fasol, and H. Kano, SPIE Proc. **1677**, 15 (1992).

[13]N. W. Ashcroft and N. D. Mermin, in *Solid State Physics: Advances in Research and Applications* (Int. ed.), edited by H. Ehrenreich and D. Turnbull (Saunders, Philadelphia, 1976).

[14]G. Harbeke, O. Madelung, and U. Rössler, in *Physics of Group IV Elements and III-V Compounds,* edited by O. Madelung, Landolt-Börnstein, New Series, Group III, Vol. 17a, Pt. 2.13.1 (Springer, Berlin, 1982).

[15]R. T. Phillips (private communication).

[16]K. L. Shaklee, M. Cardona, and F. H. Pollak, Phys. Rev. Lett. **16**, 48 (1966).

[17]J. M. Luttinger, Phys. Rev. **102**, 1030 (1956).

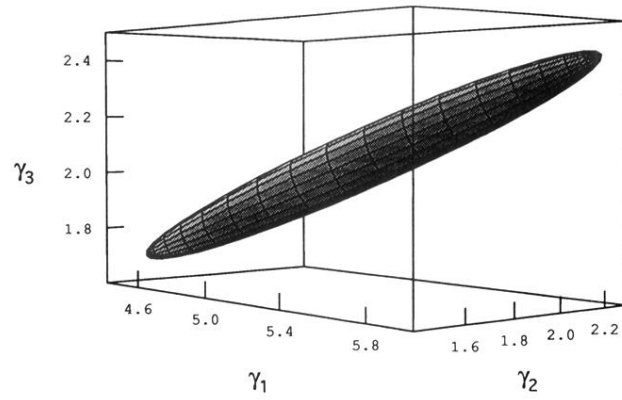[18]W. Hackenberg and H. P. Hughes, Phys. Rev. B **49**, 7990 (1994).

FIG. 4. Schematic representation of the volume in Luttinger space, where $(\gamma_1, \gamma_2, \gamma_3)$ lead to $S \leq 1$ meV, i.e., to good agreement with the HEL data. Clearly, Luttinger parameters of significantly different magnitudes do not necessarily contradict neither each other or the present HEL measurements.